Brain Research, 525 (1990) 59–70
Elsevier

BRES 15761

A morphometric analysis of isolated *Torpedo* electric organ synaptic vesicles following stimulation

G.Q. Fox, D. Kötting and G.H.C. Dowe

Max-Planck-Institut für biophysikalische Chemie, Göttingen (F.R.G.)

(Accepted 20 February 1990)

Key words: Synaptic vesicle; Sucrose gradient; Zonal centrifugation; Acetylcholine; *Torpedo* electric organ; Morphometric analysis

The electric organ of *Torpedo* has been stimulated with 1800 pulses at 0.1 Hz to produce biochemical and morphological heterogeneity of its synaptic vesicle population. This was verified by biochemical and morphometric analyses of the synaptic vesicle population isolated by sucrose density gradient zonal separation following stimulation. Biochemical or metabolic heterogeneity was verified using 2 established criteria: the appearance of a second peak of acetylcholine (ACh) in denser fractions of the zonal gradient and a corresponding overlapping peak of incorporated radiolabelled ACh. Morphologic heterogeneity was deduced by the presence in this second peak of a subclass of synaptic vesicles having a mean diameter of 68 nm i.e., a diameter 20–25% smaller than the 90 nm subclass that represents the most prominent subclass of the intact terminal population. Despite having satisfied these 3 criteria, functionally relevant heterogeneity cannot be assumed. One reason is due to our failure to recover the 90 nm subclass of vesicle which provides the physical basis to explain the 2 ACh peaks along the gradient. Because of this, the point is raised whether the stimulation-induced ACh peak is not merely an artifact due to inadequate sampling. On the other hand, radioactive labelling of the ACh pool provides a more convincing demonstration of the existence of 2 metabolically different subclasses. We conclude that morphological heterogeneity of the ACh vesicle population has never been established and that metabolic heterogeneity, as it has been studied to date, pertains to a single-sized subclass population of vesicles measuring 68 nm in diameter.

INTRODUCTION

Over the years, a vesicle-mediated mechanism has been formulated to describe acetylcholine (ACh) transmitter release from the synaptic terminals of *Torpedo* electric organ[24]. In brief, it states that stimulation directly induces the reserve synaptic vesicles to fuse with the presynaptic membrane thereby releasing their ACh. A recycling process recovers the fused vesicular membranes in the form of a dimensionally smaller (diameter reduction of 25%) vesicle subclass. This subclass so formed, refills and then can either enter into more cycles of release or enlarge back to its original size. It has come to be accepted[15] that the size of the reserve vesicles is 90 nm in diameter and that they contain approximately 2.5×10^5 molecules of ACh in the fully loaded state. This implies that the empty, recycling vesicles are in the neighborhood of 68 nm in diameter. From this, it is easy to appreciate that one of the great attractions of this system has been this promise of a functionally correlated biochemical and morphological heterogeneity.

Of late, however, some conflicting observations have been reported which, if substantiated, will necessitate a re-evaluation of this view[5–7]. One of these is the claim that the resting terminal vesicle population, rather than being composed of a single reserve size class[27,29] is actually comprised of multiple subclasses including the 2 believed involved in neurotransmission[5,6]. This challenges the concept that vesicle size is a function of stimulation. Secondly, it has been questioned whether sucrose density separation and zonal centrifugation are capable of successfully isolating the 90 nm vesicle subclass[7]. Using this standard method of isolation these investigators found the recovered ACh vesicles to belong to a single 68 nm subclass and could find no indication of the presence of a 90 nm subclass of vesicle.

Because of these problems, the present follow-up study was initiated. The intent was to examine the size distributions of isolated vesicles obtained following stimulation of the electric organ under conditions designed to promote morphological heterogeneity[29].

MATERIALS AND METHODS

Specimen preparation

One adult *Torpedo marmorata* was used in this study, obtained from the Institut de Biologie Marine, Arcachon, France. The animal was anaesthetized with 0.05% (w/v) ethyl *m*-aminobenzoate methansulfonate (MS-222) (Sigma) in sea water. One electric organ served as a control and was isolated from stimulation by severance of its 4 electromotor nerves. Stimulation of the other electric organ was by way of the appropriate electric lobe with 1800 pulses at 0.1 Hz.

Correspondence: G.Q. Fox, Max-Planck-Institut für biophysikalische Chemie, 3400 Göttingen, F.R.G.

The study consists of 3 experiments. Expt. 1 investigates the biochemical and morphological effects upon the isolated vesicle populations as a function of 1800 pulses of 0.1 Hz stimulation of whole electric organ. Expts. 2 and 3 represent extensions of this by including periods of 1 and 2 h of perfusion of isotopically labelled acetate[8,9]. The perfusion periods, however, were performed on blocks of electric organ[30] that were dissected from the whole organ following stimulation. The perfusate was a sucrose-enriched *Torpedo* Ringer's which was pumped by closed circuit through the vascular system. The perfusate contained 1.5 μCi/ml of [^{3}H]acetate (100 mCi/mmol) (New England Nuclear, Dreieich, F.R.G.) which, upon conversion to [^{3}H]ACh, served as a marker for incorporated, vesicular ACh. Determination of radioactivity was conducted as described by Giompres[8,9].

The anaesthetized animal was killed by spinal section after stimulation. Blocks (50 g) of electric organ were either stored immediately in liquid nitrogen (Expt. 1) or prepared for perfusion (as above) and then storage (Expts. 2 and 3).

Iso-osmotic fractionation and gradient preparation

Vesicles were isolated from extracts of frozen electric organ[3,22], using a continuous (0.2–0.85 M sucrose), iso-osmotic (approx. 850 mosmol) sucrose-NaCl gradient having a 1.45 M sucrose cushion. Approximately 50 g of frozen electric organ was crushed to a fine powder and the vesicles, soluble protein and small membrane fragments extracted at 4 °C in 0.4 M NaCl containing 10 mM Tris-HCl buffer and 1 mM EGTA at pH 7.0. The suspension was passed through 4 layers of cheesecloth and the filtrate centrifuged for 30 min at 12,000 *g* (10,500 rpm) on a Sorvall SS 34 rotor. The supernatant (S_{12}) was then layered on a sucrose density gradient and centrifuged in a zonal rotor (Beckman Ti 60) for 3 h at 130,000 *g* (avg. 50,000 rpm). The ACh contained in the S_{12} fraction represents total bound ACh[19]. Samples from each gradient fraction were collected for ACh and refractive indices determinations. The ACh was extracted from each sample by reducing the pH to 3.5–4.0 with HCl and freezing. The ACh was then assayed using the leech bioassay system[3,22]. Discontinuities in the curves of the ACh distributions were used as the basis for indicating the locations of the vesicle subpopulations[25,31], though all fractions contained within what came to be defined as the 'vesicle' gradient (see Results) were analyzed.

Morphological preparation of zonal gradient fractions

Samples from all gradient fractions representing the vesicular-containing region of the gradient were collected for morphological analysis. One ml of fraction was prepared by addition of an equal volume of fixative to produce a final concentration of 2% glutaraldehyde + 0.3 M sodium cacodylate buffered at pH 7.2. These were stored in fixative at 4 °C for periods of weeks with no detectable deleterious effects[7]. Following primary fixation, 4% osmium tetroxide in 0.3 M sodium cacodylate was added to produce a 1% working solution. This was allowed to fix for an additional 1 h at 4 °C. The samples were then layered on 0.45 μm Millipore filters over a circular area of 5 mm diameter using a vacuum. Each was then overlaid with a 1–3% solution of warm agar, also with the aim of a vacuum. Samples were bisected, dehydrated in ethanol and embedded in Epon 812 using propylene oxide as a transferral agent.

Morphometric analysis

To estimate the volume of each zonal sample, a 1-μm section of the 5-mm embedded pellicle was cut and stained with Toluidine blue. The pellicle was oriented so that its thickness could be measured. An ocular micrometer at 400 × magnification was used to make 10 measurements along this length, with the mean then used to calculate the pellicle volume.

Vesicle distributions were obtained by first cutting thin sections at a light gold interference color (estimated at 118 nm), mounting them unsupported on 150 mesh grids and counterstaining with uranyl acetate and lead citrate. Five to 10 micrographs were taken along the thickness of the sample at an uncorrected 24,000 × magnification. To approximate a systematic sampling routine, the region chosen for photography was located near successive grid wires. The sample positioning was done at low magnification (3,000 ×) to minimize bias. Photographic prints were made at 3 × magnification with a 15 × 15 cm reading area outlined in the center. A Zeiss particle analyzer was used to count and size all vesicle profiles located therein. To be counted the vesicle had to be circular to ovoid, membrane bound and have a lucent interior. The electron microscope was calibrated with a cross-grating replica (2160 lines/mm), the photographic enlarger with a linear rule and the particle analyzer with millimeter graph paper. From these data, size distribution curves were constructed and statistics computed. The formula: $N_v = N_a/(D + t)$[21], where N_v = number/unit volume. N_a = number/unit area. D = mean particle diameter and t = section thickness, was used throughout for density computations. It is of interest to note that a density of 10^8 vesicles/ml of sample fraction is the limit of ACh detection by the bioassay method employed.

Presentation of data

The 6 zonal gradients analyzed in this study were aligned upon the fractions having a refractive index (RI) = 1.3600. All histogram data were smoothed using a 3 point moving average. ACh values in Table I are expressed as nmol/g wet weight of tissue, whereas those in Fig. 1 as nmol/ml of zonal fraction. For more information pertaining to control distributions, the reader is referred to Fox[6,7].

RESULTS

Biochemistry

Analysis of control distributions and identification of vesicular heterogeneity

One thousand eight hundred pulses of 0.1 Hz stimulation has the general effect of fatiguing the organ's ability to produce evoked discharges, reducing them by up to 90%[30]. It also produces a marked reduction in the levels of bound ACh[27,30]. When the amounts of bound ACh obtained from each zonal fraction are plotted as a histogram distribution, a second peak often appears in the denser fractions of the gradient. If radiolabelled acetate is perfused through electric organ preparations following stimulation, in order to localize the gradient position of newly synthesized ACh, an overlap with this denser peak of ACh often occurs[19,20,31]. Together, these observations have come to be accepted as the basis upon which metabolic heterogeneity is judged. This second ACh peak has been termed 'VP_2' and is defined as being representative of a subpopulation of actively recycling, refilling vesicles[31]. This is in contrast to the ACh mode, termed 'VP_1' which represents the fully loaded reserve population. A prerequisite of this study, therefore, was first to verify that the stimulation conditions produced these 2 biochemical criteria of vesicle heterogeneity.

Table I summarizes the data pertaining to ACh levels from the 3 sets of experiments. Expt. 1 represents the condition immediately following 1800 pulses of 0.1 Hz stimulation. The control shows a content of total, bound ACh (S_{12}) of 77 nmol ACh/g of tissue. Stimulation reduced this amount by 50% to 39 nmol ACh/g. Plotting

TABLE I

Biochemical determinations

Values are ± S.D.

	Recovered amounts of ACh (nmol ACh/g)								
	S_{12}	*Peak gradient fraction amount*	*Total vesicle gradient (20–40)*	*Mean vesicle fraction*	*Total VP_1 gradient (28–30)*	*Mean VP_1 fraction*	*Total VP_2 gradient (32–36)*	*Mean VP_2 fraction*	*Mean fraction number*
Controls									
Expt. 1	77	9.4	75	3.6 ± 3.1	25.4	8.5 ± 0.8	18.0	3.6 ± 1.7	30 ± 3.5
Expt. 2	62	9.1	54	2.6 ± 2.9	24.7	8.2 ± 0.7	6.9	1.4 ± 0.9	29 ± 3.0
Expt. 3	56	8.1	54	2.6 ± 2.9	22.7	7.6 ± 1.0	7.4	1.5 ± 0.8	29 ± 3.0
Stimulated									
Expt. 1	39	2.0	20	1.0 ± 0.6	5.5	1.8 ± 0.2	5.2	1.0 ± 0.2	30 ± 4.4
Expt. 2	24	2.0	23	1.1 ± 0.7	4.8	1.6 ± 0.2	5.4	1.1 ± 0.7	28 ± 4.1
Expt. 3	23	1.6	10	0.5 ± 0.4	2.0	0.7 ± 0.1	5.1	1.0 ± 0.4	32 ± 3.7
	Recovered [^{3}H]ACh (dpm × 10^2/ml)						*Specific radioactivity (dpm × 10^2/nmol ACh)*		
	S_{12}	*Total vesicle gradient*	*Mean vesicle fraction*	*Mean VP_1 fraction*	*Mean VP_2 fraction*	*Mean fraction number*	*Mean vesicle fraction*	*Mean VP_1 fraction*	*Mean VP_2 fraction*
Controls									
Expt. 2	2553	1140	54 ± 26	104 ± 17	50 ± 7	30 ± 5.7	6 ± 6.8	1 ± 0.2	4 ± 2.9
Expt. 3	11270	4081	194 ± 144	391 ± 2	276 ± 92	30 ± 4.0	14 ± 10	5 ± 0.7	19 ± 5.6
Stimulated									
Expt. 2	1391	823	39 ± 26	50 ± 14	67 ± 22	30 ± 4.5	4 ± 3.3	2 ± 0.9	6 ± 3.3
Expt. 3	3901	2514	120 ± 108	138 ± 38	260 ± 116	31 ± 4.1	23 ± 6.0	16 ± 1.5	20 ± 2.2
	Vesicle molarity (nmol ACh/68 nm vesicle)			*Vesicle ACh content (ACh molecules × 10^5/vesicle)*		
	Vesicle	*VP_1*	*VP_2*	*Vesicle*	*VP_1*	*VP_2*			
Controls									
Expt. 1	1.8 ± 1.2	3.2 ± 0.3	1.5 ± 0.4	1.7 ± 1.0	3.1 ± 0.3	1.5 ± 0.3			
Expt. 2	2.1 ± 1.2	3.2 ± 1.0	1.5 ± 0.4	1.6 ± 0.9	2.6 ± 0.9	1.1 ± 0.5			
Expt. 3	1.4 ± 1.5	3.0 ± 0.9	0.7 ± 0.5	1.1 ± 1.1	2.4 ± 0.4	0.6 ± 0.3			
Stimulated									
Expt. 1	10 ± 11	21 ± 17	14 ± 14	9.3 ± 8.8	18 ± 14	11 ± 11			
Expt. 2	1.3 ± 1.1	2.4 ± 1.0	1.0 ± 0.6	1.2 ± 0.9	2.0 ± 0.8	0.9 ± 0.5			
Expt. 3	1.4 ± 1.1	1.7 ± 0.5	3.0 ± 0.5	1.2 ± 1.0	1.3 ± 0.4	2.8 ± 0.4			

the ACh amounts from each zonal fraction produces a normal curve for control and a flattened, bimodal curve for the stimulated preparation (Fig. 1). The mode fraction 30 of the control curve contains 9.4 nmol ACh/g (Table I). The ACh distribution of the stimulated preparation has peaks at fractions 29 (2.0 nmol ACh/g) and 35 (1.3 nmol ACh/g) (Fig. 1, Table I). Fraction 30 is the mean for both curves (Table I, mean fraction number). The 2 curves extend long tails into the less dense regions of the gradient (to fraction 6 in this experiment). Electron microscopy has revealed that fractions up to about number 15 are essentially devoid of organelles, supporting the contention that this ACh is derived from the soluble, cytoplasmic pool[1,22]. On the other hand, no esterase inhibitors were employed in this study, which argues for it being of the bound form[19].

Similar ACh results were obtained from Expt. 2 which consisted of identical stimulation conditions plus 1 h of perfusion. The control value for total, bound ACh was 62 nmol ACh/g which then fell to 24 nmol ACh/g after stimulation and perfusion (Table I). The ACh distributes along the zonal gradient similar to that seen in Expt. 1 (Fig. 1). Control values describe a normal curve having a mode at fraction 29 (9.1 nmol ACh/g). The distribution of the stimulated condition is also flattened and bimodal with peaks at fractions 26 and 27 (2.0 nmol ACh/g) and 32 (1.9 nmol ACh/g). No significant difference between the fraction means of the control and stimulated curves was present (Table I).

A bimodal distribution of radiolabelled ACh having a major mode at fraction 29 and a minor mode at fraction 37 was obtained from the control of this experiment (Fig.

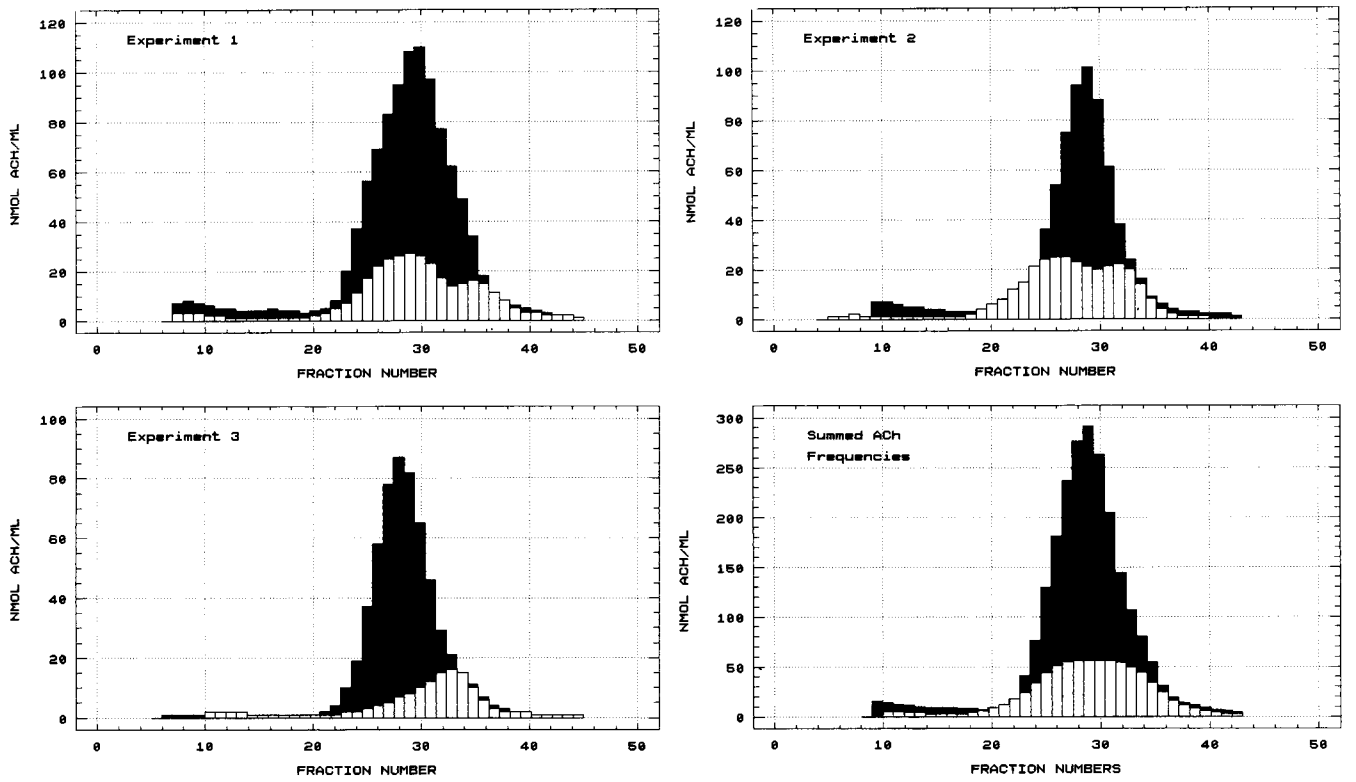

Fig. 1. ACh distribution curves of data obtained from the 3 experiments. Solid black bars represent control and non-filled white bars stimulated. The ordinate expresses amount of ACh recovered from 1 ml of gradient fraction. (Note that the values in Table I have been converted to amount/g wet weight of tissue.). Expt. 1 illustrates ACh distributions following 1800 pulses of 0.1 Hz stimulation. The control curve is normal in form (excepting the long tail into the less dense (lower numbered fractions) and the stimulated bimodal. Vesicle-containing fractions are from 20–40. The VP_1 modes of both curves are at fractions 29 and 30. The minor mode of the stimulated curve (fraction 35) represents the VP_2 fraction. Expt. 2 shows a similar ACh distribution with the major (VP_1) and minor (VP_2) modes of the stimulated distribution shifted slightly towards the left into the less-dense fractions. Expt. 3 shows the control ACh distribution to be positively skewed with its VP_1 mode at fraction 28. The stimulation condition has a distribution with a single VP_2 mode at fraction 33. Summation of these data from the 3 experiments produces 2 overlapping normal curves. This illustrates that the discreteness of the VP_2 discontinuity is heavily influenced by variations in frequencies.

2A). In contrast, stimulation produced a mirror image of this distribution by having its major mode in the denser fraction 34 and its minor mode in the lighter fraction 28 (Fig. 2A). Both curves show their highest levels of radioactivity in the lightest fractions.

Expt. 3, which was stimulated, then perfused for 2 h, shows total, bound ACh to have declined from 56 to 23 nmol ACh/g (Table I). The control curve remains normal with its mode at fraction 28 (8.1 nmol ACh/g), whereas the stimulation curve is negatively skewed, having but a single mode at fraction 33 (1.6 nmol ACh/g) (Fig. 1).

Distribution of bound [^{3}H]ACh in the control is also bimodal with modes at fractions 29 and 34 (Fig. 2B). The stimulated preparation produced a distribution having a single mode at fraction 33 (Fig. 2B). Again both curves show high levels of radioactivity in the lightest fractions of the gradient.

Based on these data above, we conclude that the secondary peaks of ACh appearing in the denser fractions of the gradients from the stimulated preparations, together with the overlapping modes of bound [^{3}H]ACh, satisfy the criteria defining metabolic heterogeneity[1, 8,9,19,29].

Therefore, for purposes of further analysis we define the overall vesicular region of each ACh gradient (termed Vesicle) as being represented by fractions 20–40. Of the 6 gradients represented, a mean refractive index (RI) of 1.3593 ± 0.0009 was determined over a range of 1.3490–1.3792, equivalent to a sucrose density range of 0.6 M at iso-osmolarity. The VP, vesicle-containing region of each gradient is given by fractions 28–30 with a mean RI = 1.3569 ± 0.0005 and an equivalent sucrose density of 0.39 M. Fractions 32–36 represent the VP_2 region of the gradient with a mean RI of 1.3615 ± 0.0006, and an equivalent sucrose density of 0.55 M sucrose (for comparisons see Agoston[1] and Whittaker[26]).

Effect of stimulation on the Vesicle, VP_1 and VP_2 fractions

Table I also itemizes the ACh data in terms of the 3 components groups: Vesicle, VP_1 and VP_2. Of these, the

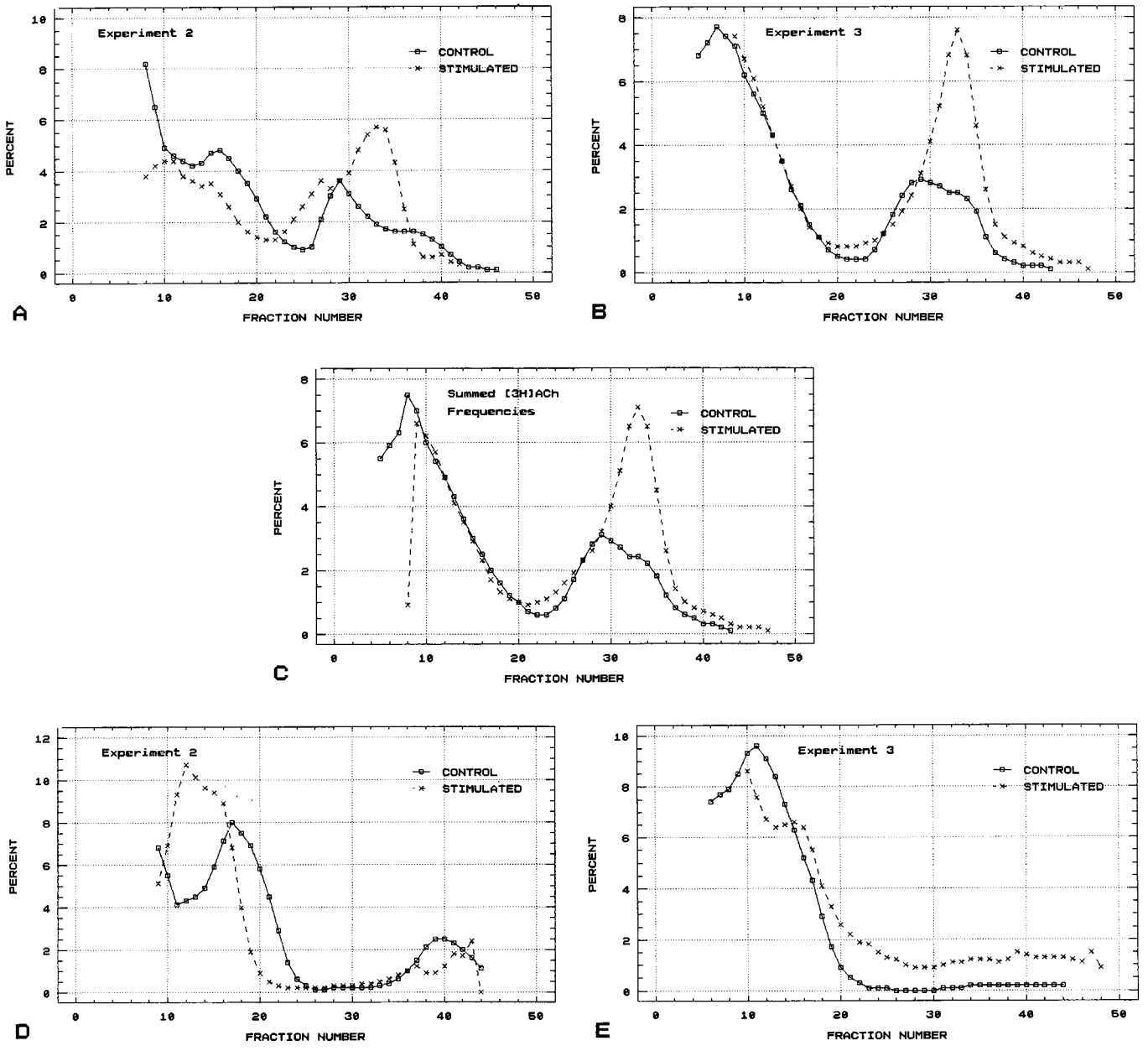

Fig. 2. Radiolabelled ACh and specific radioactivity (SRA) distribution curves of Expts. 2 and 3. A: Expt. 2 shows both control and stimulated distributions to be multimodal. The portion over the vesicle-containing region of the gradient (20–40) is bimodal with the 2 modes overlying the VP_1 and VP_2 peaks of the ACh distribution of Fig. 1 above. The control and stimulated curves appear to be mirror images of each other. There is a considerable presence of radioactivity in the soluble region of the gradient but agreement is divided over whether this represents labelled acetate or ACh. B: Expt. 3 is closely similar to Expt. 2. The control curve is bimodal over the vesicle-containing region of the gradient. The stimulated curve has a single mode in the VP_2 region. C: summation of the frequencies of these 2 experiments produces overlapping curves. The control curve is positively skewed and can be seen to have lost the bimodality of its component curves. It still has a mode at fraction 29, in contrast to fraction 33 of the stimulated condition. The 2 curves are interpreted as representing the same population of VP_2 vesicles. D: computed SRA ratios from the data of Expt. 2. The distribution of both curves is vaguely U-shaped with the peak values of the dense fractions showing poor registration with the VP_2 region of the gradient (mode at fraction 33) (compare with Expt. 2 of Fig. 1). E: SRA values from data of Expt. 3. Both of the curves are heavily skewed out of the soluble fractions and give no indication of a vesicular-related component (compare with Expt. 3 of Fig. 1). The greatest ratios are computed from the soluble regions of the gradients, which are devoid of organelles.

VP_1 fractions experienced the most dramatic stimulation-induced declines from a high of 8.5 to a low of 0.7 nmol/g (Table I, mean VP_1). VP_2s, in contrast, appeared stabilized at about 1–1.5 nmol/g (with the exception of the control from Expt. 1!). Mean ACh levels were not significantly effected by the 2 perfusion periods included in Expts. 2 and 3 (Table I), thus the values from all 3 stimulated conditions can be considered comparable. Summing them in order to examine the reproducibility of the stimulation-induced VP_2 mode resulted in a normal

curve having good registration with the controls (Fig. 1). This suggests that the multiple ACh peaks may be due to sampling error rather than to a functionally induced event. In a similar fashion, the summing of the [^{3}H]ACh frequencies (Expts. 2 and 3) produces the distribution curves seen in Fig. 2C. The control curve is now positively skewed retaining only a slight suggestion of the bimodal character of the individual curves. The stimulated distribution completely subsumes the control data, suggesting both curves to be representative of the same population. Its mode at fraction 33 indicates it to be localized within the VP_2 region of the gradient.

Specific radioactivity computations

Computations of specific radioactivities (SRA) (dpm of [^{3}H]ACh/nmol ACh/g) were performed to evaluate the uptake potential of the 3 vesicle groups (Table I). The VP_2 ratios, as anticipated, consistently exceeded their corresponding VP_1 ratios by up to 4 times, but did so equally for controls and stimulated preparations, indicating them to be independent of stimulation (Table I). Additionally, these distributions co-localized poorly with any vesicle-containing groups within the ACh gradient (Fig. 2D,E). In Expt. 2, both control and stimulated SRA curves were U-shaped with the denser SRA peaks developing in gradient fractions beyond those representing the VP_2 vesicles (Fig. 2D). In Expt. 3, the 2 curves were highly skewed into the denser fractions with uniformly low ratios across most of the entirety of the Vesicle portion of both gradients (Fig. 2E), and this despite the existence of a distinct peak of [^{3}H]ACh in the VP_2 region (Fig. 2B). The largest ratios came from the lighter, soluble fractions of all gradients. These curves indicate that the vesicles within the defined Vesicle region of the gradient are not actively involved in the uptake of isotopically labelled ACh.

To briefly summarize, stimulation without or with accompanying perfusion produced similar overall declines in total, bound ACh. Distributions of bound ACh across the Vesicle fractions of the gradients from stimulated preparations showed the formation of additional peaks. Because these peaks remained within the confines of their control curves, their appearance is due to declining levels of ACh. Incorporation of [^{3}H]ACh occurred in the VP_2 region of the gradient but SRA computations failed to verify any preferential ACh uptake by these vesicles.

Morphological distributions

Qualitative observations

A morphometric analysis of vesicles was conducted on the Vesicle fractions of the 6 ACh gradients examined. Qualitatively, the modal ACh fractions were clearly the purest in vesicular content with the amount of membranous and particulate contamination increasing in either direction (Fig. 3).

Quantitative observations

Vesicle size. Mean vesicle diameters between 63 and 73 nm were obtained for the fractions measured from the control gradient of Expt. 1 (Fig. 4). The Vesicle group measured 67 ± 3.2 nm, VP_1s, 67 ± 1.7 nm and VP_2s, 68 ± 2.4 nm (Table II). Stimulation produced a U-shaped distribution consisting of a central region of 60–70 nm vesicles bounded on either side by increasingly larger vesicles reaching 80+ nm in diameter (Fig. 4). The Vesicle group had a mean of 70 ± 7.1 nm, the VP_1s 64 ± 1.6 nm and the VP_2s 64 ± 5.2 nm (Table II). Combining and normalizing all mean fraction sizes resulted in 2 coincident, normal distributions with modes of 68 nm (Fig. 4). There was no indication of the presence of a subclass of 90 nm vesicles, though low frequencies of 90 nm vesicles were, of course, recorded (Fig. 4).

Control vesicle diameters from Expt. 2 ranged between 57 and 68 nm with means between 60 and 63 nm established for the 3 groups (Fig. 4, Table II). Stimulation produced vesicle diameters having a range of 62–78 nm with VP_1 and VP_2 means of 65 and 68 nm (Fig. 4, Table II). The combined, normalized distributions of these 2 preparations also gave coincident, normal curves, similar to that found for Expt. 1, with modes at 65 nm (Fig. 4).

Expt. 3 reiterates these results. The control gradient contained vesicles of 61–77 nm with VP_1 and VP_2 means of 64–69 nm (Fig. 4, Table II). Stimulation produced vesicle diameters ranging from 65 to 82 nm with slightly larger VP_1 and VP_2 mean diameters of 72–78 nm (Fig. 4, Table II). A slight tendency towards larger diameters in the direction of increasing gradient densities was present (Fig. 4). The combined, normalized curves of this experiment again show coincidence between both normal distributions with modes at 70 nm (Fig. 4).

To summarize, no significant differences in size were found between control and stimulated vesicles (66 and 70 nm, respectively) (Table II), nor was there any indication that the vesicles located in the VP_1 and VP_2 fractions of any of the gradients belonged to different size classes. Furthermore, no 90 nm subclass was found. Morphological heterogeneity, therefore, could not be substantiated despite the presence of the size class that heretofore defined its presence. A linear correlation between vesicle size and gradient density produced a coefficient of 0.6, counter to earlier indications that the heavier VP_2 vesicles were dimensionally smaller[31]. Together, these data show that the vesicles located throughout the Vesicle range of the ACh gradient and including those contained

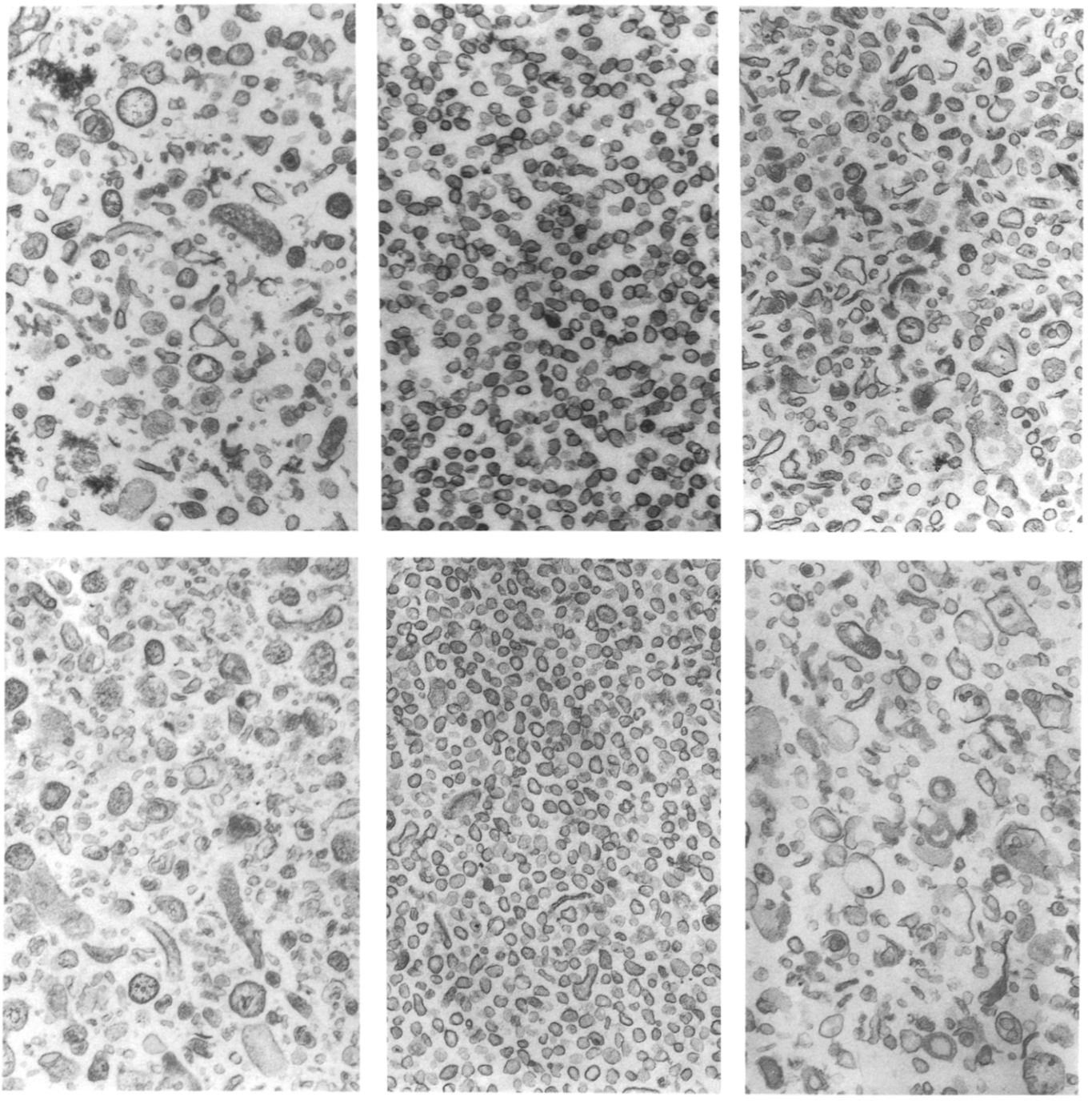

Fig. 3. Electron micrographs spanning the Vesicle gradient fractions from Expt. 2. Top row is control and the bottom row stimulated. The left column shows fractions 22 and 19, respectively, the middle column VP_1 fractions 29 and 28 and the right column fractions 37 and 36. Particulate and membranous heterogeneity increases steadily away from the 'pure' central fractions. Magnification × 30,503; 1 mm = 45.7 nm.

in fractions designated as VP_1 and VP_2, belong to a single 68 nm subclass.

Vesicle number. Stimulation produced declines in the estimated total mean number of vesicles/ml of fraction with VP_1 vesicles the most heavily effected (Table II). In no case were the VP_2 vesicle numbers from stimulated preparations found to exceed those of controls, thus ruling out concomitant recycling. Normalization of these data shows that stimulation reduced the number of VP_1 vesicles/fraction by a significant 24% ($P < 0.05$; Student's *t*-test), from 8.3 to 6.3% of total ACh vesicles, whereas VP_2 vesicles/fraction increased non-significantly by 11.5%, from 5.2 to 5.8% (Table II). These figures indicate that the perfusion periods had no quantitative effect upon vesicle numbers. They indicate further that VP_2s remain unaffected by the experimental protocol.

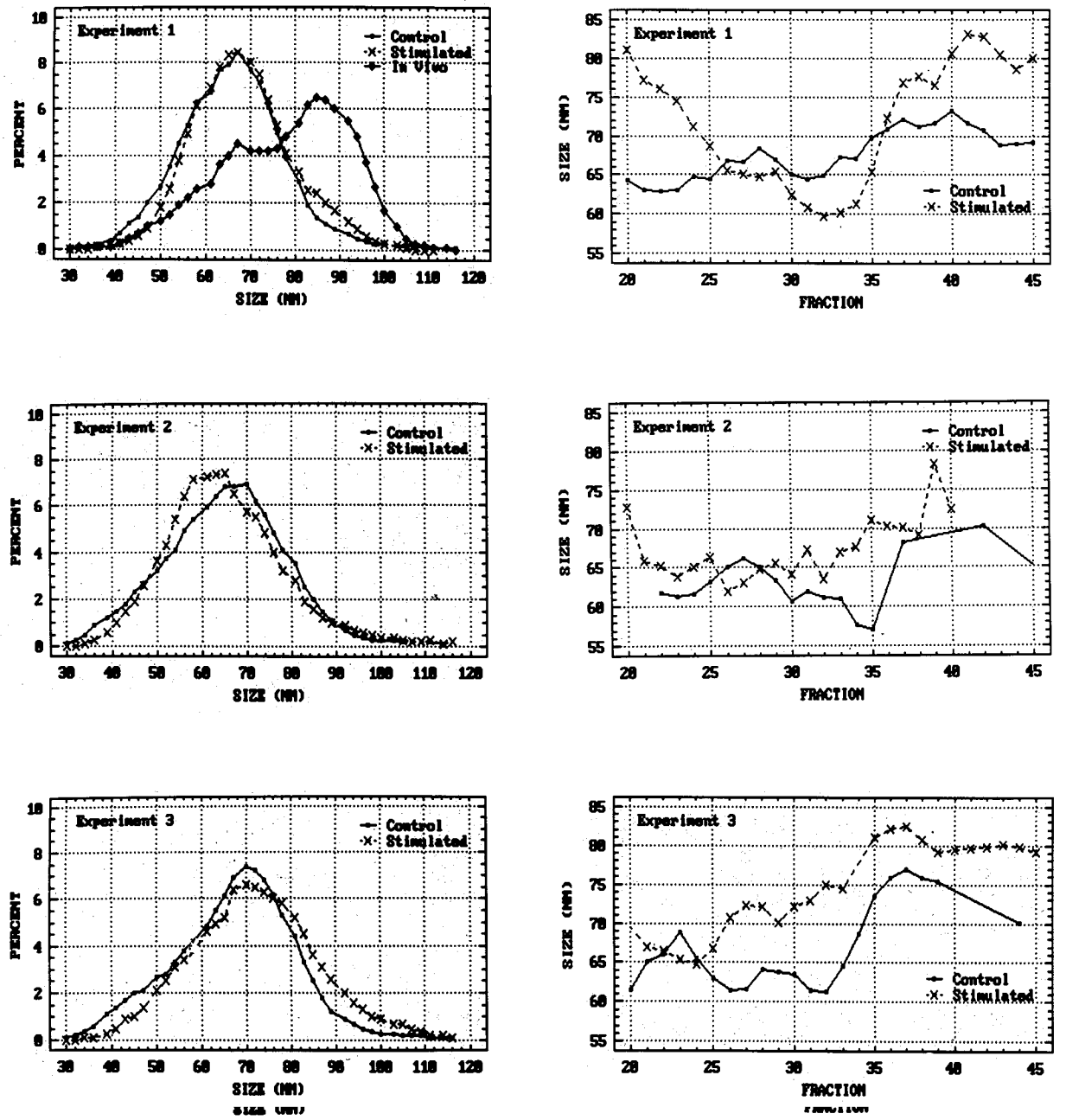

Fig. 4. Distributions of vesicle size determinations. The left column illustrates the distributions obtained when all the fraction mean sizes are pooled to reveal their representation in the total recovered vesicle population. Normal curves are generated with modes between 66 and 70 nm. Note in Expt. 1 that the 90 nm subclass of the overlying in vivo distribution is absent in all 3 experiments. The right column gives mean vesicle sizes for each fraction sample across the gradient. In general, it can be noted that the vesicle sizes within fractions 20–40 fall between 60 and 80 nm.

ACh content per vesicle. With the above data, ACh content/vesicle was computed (Table I). The values for the stimulated half of Expt. 1 were exceptionally high, due apparently to somewhat low vesicle numbers (Table II). They have been left out of the following considerations which are based on the other 5 gradients. For the 3 control experiments, molarities averaging 1.6 ± 1.2 were obtained for a vesicle having a 68 nm o.d. and a 6 nm plasma membrane[7]. This amounts to 1.3 × 10^5 molecules of ACh/vesicle. The differences between VP_1 and VP_2 molarities were significant for control but not stimulated vesicles.

It should be noted that the curves upon which these values are derived are dissimilar. ACh curves are normal in form whereas vesicle number curves are positively skewed. These latter curves additionally have an inherent tendency towards increasing vesicular heterogeneity in both directions away from the mode. As our counts include all vesicle profiles (as defined in Materials and Methods), they become increasingly biased towards

TABLE II

Morphometric determinations

Values are ± S.D.

	Vesicle size (nm)			*Vesicle number × 10^9/ml*			*As percent of vesicle gradient*		*Mean fraction number*
	Vesicle	*VP_1*	*VP_2*	*Vesicle*	*VP_1*	*VP_2*	*VP_1*	*VP_2*	
Controls									
Expt. 1	67 ± 3.2	67 ± 1.7	68 ± 2.4	148 ± 95	216 ± 43	197 ± 115	7.0	6.2	30 ± 4.6
Expt. 2	62 ± 3.0	63 ± 2.2	60 ± 2.1	142 ± 78	257 ± 93	107 ± 23	10.8	4.4	29 ± 3.6
Expt. 3	67 ± 5.6	64 ± 0.3	69 ± 6.0	159 ± 70	212 ± 57	157 ± 45	7.0	5.2	31 ± 5.4
Mean	66 ± 4.6						8.3 ± 2.2	5.2 ± 0.9	
Stimulated									
Expt. 1	70 ± 7.1	64 ± 1.6	64 ± 5.2	17 ± 24	12 ± 6	14 ± 11	7.1	5.9	31 ± 4.3
Expt. 2	67 ± 4.0	65 ± 0.7	68 ± 3.0	75 ± 26	68 ± 20	95 ± 45	6.2	7.6	30 ± 5.8
Expt. 3	73 ± 5.9	72 ± 1.2	78 ± 4.0	41 ± 30	39 ± 7	27 ± 14	5.3	4.0	34 ± 5.4
Mean	70 ± 6.2						6.3 ± 0.9	5.8 ± 1.8	

	Specific radioactivity/vesicle (dpm × 10^{-8}/vesicle)			*Molecular uptake (molecules/vesicle)*		
	Vesicle	*VP_1*	*VP_2*	*Vesicle*	*VP_1*	*VP_2*
Controls						
Expt. 2	4 ± 2.3	4 ± 1.8	5 ± 1.1	121 ± 64	123 ± 50	136 ± 30
Expt. 3	13 ± 8.6	19 ± 5.3	19 ± 8.7	367 ± 236	529 ± 144	530 ± 236
Stimulated						
Expt. 2	6 ± 4.2	8 ± 3.0	9 ± 5.6	151 ± 114	211 ± 82	243 ± 153
Expt. 3	41 ± 32	36 ± 13	87 ± 18	1107 ± 862	993 ± 335	2388 ± 491

numerical overestimation away from the mode which, in turn, leads to underestimates of ACh content. Because of this, the control mode values are regarded as being the most reliable. They indicate that the 68 nm vesicle subclass contains, on average, a 2.7 M solution of ACh representing 2.3 × 10^5 molecules. In either case, both sets of values greatly exceed a quantal size estimated to be 7000 molecules[4].

[^{3}H]ACh uptake per vesicle. Calculation of the amount of [^{3}H]ACh/vesicle provides a direct means by which to estimate vesicular uptake of newly synthesized ACh (Specific radioactivity/vesicle) (Table II). Mean values, whether from control or stimulated preparations or from Vesicle, VP_1 and VP_2 gradient fractions, showed time-dependent uptake from 10^{-8} to 10^{-7} dpm/vesicle over the 1 h difference in perfusion times, equivalent to 1 labelled ACh molecule/10^7–10^6 vesicles or 4000 presynaptic terminals (based on data from Kriebel[11]). This amounts to 10^2–10^3 molecules/labelled vesicle (Molecular uptake, Table II). Vesicles in the VP_1 region showed a doubling of uptake by the second hour of perfusion, whereas those in the VP_2 fractions increased by a factor of 4.

DISCUSSION

The intent of this study has been to reconfirm the claim that morphological heterogeneity can be functionally induced within the ACh vesicle population of *Torpedo* electric organ. Indication of this possibility was first demonstrated by Zimmermann and Whittaker[27] when they showed that in situ stimulation caused a shift in the size mode of the terminal vesicle population from 75 to 55 nm. As this was accompanied by a substantial drop in ACh and ATP, these 2 sizes were suspected of representing 2 metabolic states of vesicle, namely reserve and recycling. The initial attempts to examine this suspected biochemical heterogeneity using sucrose density separation and zonal centrifugation proved to be unsuccessful[27], prompting a change in approach to one using blocks of electric organ in place of the intact, whole electric organs; a method which also proved to be better suited for the introduction of putative vesicular markers[30,31]. This approach showed that it was now possible to obtain multiple peaks of ACh and ATP, which appeared to correlate with the 2 vesicle size classes[31]. Part of this argument rested on the demonstration that vesicles could be loaded with dextran and that most of them so labelled were of the smaller size[30]. From this, it came to be accepted that the 2 peaks of ACh (VP_1 and VP_2) corresponded to the large and small vesicle size classes respectively, thus indicating both a functionally induced metabolic and morphologic heterogeneity. The vesicles within the VP_1 peak fraction represented the filled vesicle at rest and measured 90 nm in diameter. The VP_2 vesicles

were partially filled and in a recycling state and were 25% smaller (i.e. approximately 68 nm). Further support for this interpretation was provided by the demonstration that the more dense, stimulation-induced VP_2 peak coincided with a peak of incorporated [^{3}H]ACh[31]. This has been regarded as showing that the vesicles contained in these heavier fractions are more dynamically involved in the uptake process because SRA ratios were shown to greatly exceed those obtained for VP_1s[31]. This series of observations, showing a stimulation-induced 20–25% difference in vesicle size, 2 density peaks of ACh, and an overlapping peak of incorporated [^{3}H]ACh with the denser VP_2 peak, form the basis by which morphologic and metabolic heterogeneity have been judged in this system to date.

In this study we stimulated the whole organ with 1800 pulses at 0.1 Hz and then in 2 experiments followed that with in block perfusion of [^{3}H]acetate for 1 and 2 h, a further modification that has also been found to produce the desired heterogeneity[1]. We have satisfied ourselves that the criteria defining metabolic heterogeneity have been met, namely that a second peak of ACh in denser regions of the gradient has been generated and that it coincides with a peak of incorporated [^{3}H]ACh. On the other hand, morphologic heterogeneity, although inferred by the presence of 68 nm vesicles within these denser fractions, was not demonstrated because of our failure to locate the 90 nm subclass.

The significant finding of this study, therefore, has been to show that the vesicles contained within all the ACh fractions, including those specifically identified as representing VP_1 and VP_2 populations, are from a single size class having a mean diameter of 68 nm, and this regardless of the experimental condition[2,7,10]. The causes for the failure to isolate the 90 nm subclass remain unknown though shrinkage due to osmotic effects from any or all of the preparative steps has been ruled out[7]. Freezing damage has also been suggested[7], but has yet to be demonstrated. The 90 nm subclass is present in synaptosome preparations and has been partially recovered, using another gradient system[7]. As our numerical calculations show substantial losses of vesicles occurring following stimulation, it would appear that the 90 nm subclass is being selectively eliminated by this method of isolation[7].

This failure redirects one's attention to how the concept of a 90 nm subclass came into being prior to Fox's 1988 morphometric demonstration[6]. Mean values of vesicle distributions from intact terminal populations have been variously reported to lie somewhere between 60 and 90 nm[13,14,27]. Isolated, negatively stained vesicles have been measured at 122 nm[16] and 81 nm[17]. In the study where isolated vesicle distributions from both control and stimulated preparations were first reported[31], VP_1 vesicles were only 'approximated' at 90 nm and no dimension was given for the VP_2s from the denser gradient fractions, despite the inclusion of supportive histograms. Thereafter, 90 nm became the generally accepted VP_1 dimension[9,15], despite the necessity of now having to incorporate an inappropriate correction factor to achieve this figure[15]. Taking into account that many of these studies failed to correct for measurement error (e.g. reader and magnification) still does not allow one to conclude that a single size class of 90 nm vesicles exists, let alone that it has been successfully recovered in isolated form by the methods described[7].

But having said this, one is then further obliged to re-examine the concept of metabolic heterogeneity, as it was formulated, in part, to explain the size differences that were first observed in the in situ vesicle distributions[27,28]. By failing to demonstrate size differences in the isolated ACh population, the physical basis upon which metabolic heterogeneity has heretofore depended is lost[19] and we are faced with the problem of accounting for the migration of a presumed partially filled vesicle of unitary dimension into the denser gradient fractions. As noted above, stimulation-induced metabolic heterogeneity is, in part, defined by the presence of the VP_2 ACh peak in the denser fractions of the gradient. In our distributions, this peak appears as a result of falling levels of ACh. This poses the question of whether the amount of ACh recovered/fraction is of a statistically representative size; the analogy being that of throwing a pair of dice a sufficient number of times to get a classic Gaussian distribution. We have found that considerable variability can be expected with regards to both the appearance of the VP_2 peak (e.g. Fig. 2B[29]; Fig. 3[19]; Fig. 1[9]) and its spatial resolution[1,23]. One means of examining the significance of this peak was to sum the fraction frequencies from the 3 distribitions (Fig. 1). This resulted in the loss of the VP_2 peak into a normal curve indistinguishable from the control. Although variance between fractions might well account for this, alignment of the data was near-optimal at fraction 33 (RI =1.3600), the beginning of the designated VP_2 gradient. From this we are led to conclude that the variations seen in these ACh distributions have little functional significance.

Metabolic heterogeneity has also been argued from considerations pertaining to the incorporation of isotopically labelled ACh and the SRA ratios that can be derived therefrom[12,19,30]. We obtained [^{3}H]ACh curves which we regard as being both qualitatively and quantitatively typical to those reported earlier[19,31], and, in general, found that the VP_1 and VP_2 modes of these curves correlated well with those of the ACh distributions. The summed frequencies of these distributions,

however, gave persuasive indication that [^{3}H]ACh was localized over the VP_2 region of the gradient[9]. This can be interpreted to mean that the individual control distributions, despite showing [^{3}H]ACh modes in the VP_1 region, might properly be regarded as belonging solely to the VP_2 region of the gradient. This would resolve the paradox of how the presumably completely filled VP_1 vesicle can seemingly be able to still incorporate ACh.

On the other hand, the SRA ratios computed from these data showed surprisingly poor registration with any vesicle-containing fractions and, most notably, the VP_2 fractions. Thus, no vesicle fraction showed a reproducible active uptake of labelled ACh. We regard this as indication that the variance in this method of analysis exceeds the resolution required of it. The reader is left to decide which of these 2 closely related approaches holds the most significance. We should also mention as a final point that we could not find any indication of a third subclass of vesicle, termed the VP_0s, which has been identified in gradient fractions lighter than the VP_1s[18].

Our data indicate that ACh vesicles belong to a single size class measuring 68 nm in diameter. Along with ACh levels, they can be substantially depleted by long-term, low-frequency stimulation. The variations in distributions of ACh that occur as a result of this treatment are not considered to be indicative of metabolic processes within this population of vesicles. An indication of metabolic heterogeneity was found by radiolabelling the ACh pool, but this was lost from subsequent SRA computations. The dominant in vivo subclass of 90 nm vesicles remains unaccounted for.

Acknowledgements. The authors would like to thank Dr. P. Giompres for his assistance in the stimulation and perfusion of the animal and for performing the radiolabelled assay. He, along with Drs. J. Rylett, H. Stadler, and E. Borroni are also thanked for their participation in many lively discussions over the data and their help in critiquing the manuscript.

REFERENCES

1 Agoston, D.V., Dowe, G.H.C., Fiedler, W., Giompres, P.E., Roed, I.S., Walker, J.H., Whittaker, V.P. and Yamaguchi, T., A kinetic study of stimulus-induced vesicle recycling in electromotor nerve terminals using labile and stable vesicle markers, *J. Neurochem.*, 47 (1986) 1584–1592.
2 Agoston, D.V., Dowe, G.H.C. and Whittaker, V.P., Isolation and characterization of secretory granules storing a vasoactive intestinal polypeptide-like peptide in *Torpedo* cholinergic electromotor neurones, *J. Neurochem.*, 52 (1989) 1729–1740.
3 Dowdall, M.J., Boyne, A.F. and Whittaker, V.P., Adenosine triphosphate, a constituent of cholinergic synaptic vesicles, *Biochem. J.*, 140 (1974) 1–12.
4 Dunant, Y. and Muller, D., Quantal release of acetylcholine evoked by focal depolarization at the *Torpedo* nerve-electroplaque junction, *J. Physiol.*, 379 (1986) 461–478.
5 Fox, G.Q., Kriebel, M.E. and Kötting, D., Synaptic vesicle populations and classes of quanta in *Torpedo* and skate electric organ and muscle. In H. Zimmermann (Ed.), *Cellular and Molecular Basis of Synaptic Transmission, NATO ASI series, Vol. H21,* Springer, F.R.G., 1988, pp. 83–96.
6 Fox, G.Q., A morphometric analysis of synaptic vesicle distributions, *Brain Research,* 475 (1988) 103–117.
7 Fox, G.Q., Kötting, D. and Dowe, G.H.C., A morphometric analysis of *Torpedo* synaptic vesicles isolated by iso-osmotic sucrose gradient separations, *Brain Research,* 498 (1989) 279–288.
8 Giompres, P.E., Zimmermann, H. and Whittaker, V.P., Purification of small dense vesicles from stimulated *Torpedo* electric tissue by glass bead column chromatography, *Neuroscience,* 6 (1981) 765–774.
9 Giompres, P.E., Zimmermann, H. and Whittaker, V.P., Changes in the biochemical and biophysical parameters of cholinergic synaptic vesicles on transmitter release and during a subsequent period of rest, *Neuroscience,* 6 (1981) 775–785.
10 Kiene, M.-L. and Stadler, H., Synaptic vesicles in electromotoneurones. I. Axonal transport, site of transmitter uptake and processing of a core proteoglycan during maturation, *EMBO J.*, 6 (1987) 2209–2215.
11 Kriebel, M.E., Fox, G.Q. and Kötting, D., Effect of nerve stimulation, K^+ saline and hypertonic saline on classes of quanta, quantal content and synaptic vesicle size distribution of *Torpedo* electric organ. In H. Zimmermann (Ed.), *Cellular and Molecular Basis of Synaptic Transmission, NATO ASI series, Vol. H21,* Springer, F.R.G., 1988, pp. 97–120.
12 Marchbanks, R.M. and Israel, M., The heterogeneity of bound acetylcholine and synaptic vesicles, *Biochem. J.*, 129 (1972) 1049–1061.
13 Naef, W. and Waser, P.G., Changes in cholinergic synapses of *Torpedo* under the influence of drugs. In P.G. Waser (Ed.), *Cholinergic Mechanisms,* Raven, New York, 1975.
14 Naef, W., Munz, K. and Waser, P.G., Morphometric analyses of the electric organ of *Torpedo*: the influence of different fixative modes on the vesicle diameter, *Histochemistry,* 58 (1978) 193–201.
15 Ohsawa, K., Dowe, G.H.C., Morris, S.J. and Whittaker, V.P., The lipid and protein content of cholinergic synaptic vesicles from the electric organ of *Torpedo marmorata* purified to constant composition: implications for vesicle structure, *Brain Research,* 161 (1979) 447–457.
16 Sheridan, M.N., Whittaker, V.P. and Israel, M., The subcellular fractionation of the electric organ of *Torpedo*, *Zeit. Zellforsch.*, 74 (1966) 291–307.
17 Soifer, D. and Whittaker, V.P., Morphology of subcellular fractions derived from the electric organ of *Torpedo*, *Biochem. J.*, 128 (1972) 845–846.
18 Stadler, H. and Kiene, M.-L., Synaptic vesicles in electromotoneurones. II. Heterogeneity of populations is expressed in uptake properties: exocytosis and insertion of a core proteoglycan into the extracellular matrix, *EMBO J.*, 6 (1987) 2217–2221.
19 Suszkiw, J.B., Zimmermann, H. and Whittaker, V.P., Vesicular storage and release of acetylcholine in *Torpedo* electroplaque synapses, *J. Neurochem.*, 30 (1978) 1269–1280.
20 Suszkiw, J.B. and Whittaker, V.P., Role of vesicle recycling in vesicular storage and release of acetylcholine in *Torpedo* electroplaque synapses, *Progr. Brain Res.*, 49 (1979) 153–162.
21 Weibel, E.R., *Stereological Methods, Vol. 1,* Academic Press, London, 1979, 415 pp.
22 Whittaker, V.P., Essman, W.B. and Dowe, G.H.C., The isolation of pure cholinergic synaptic vesicles from the electric organs of elasmobranch fish of the family Torpedinidae, *Biochem. J.*, 128 (1972) 833–846.
23 Whittaker, V.P., The structure and function of cholinergic synaptic vesicles, *Biochem. Soc. Trans.*, 12 (1984) 561–576.
24 Whittaker, V.P. and Schmid, D.W., Model cholinergic systems:

the electromotor system of *Torpedo*. In V.P. Whittaker (Ed.), *The Cholinergic Synapse,* Springer, F.R.G., 1988, pp. 23–39.
25 Whittaker, V.P., The cellular basis of synaptic transmission: an overview. In H. Zimmermann (Ed.), *Cellular and Molecular Basis of Synaptic Transmisson, NATO ASI series, Vol. H21,* Springer, F.R.G., 1988, pp. 1–23.
26 Whittaker, V.P., Cholinergic synaptic vesicles are metabolically and biophysically heterogeneous even in resting terminals, *Brain Research,* 511 (1990) 113–121.
27 Zimmermann, H. and Whittaker, V.P., Effect of electrical stimulation on the yield and composition of synaptic vesicles from the cholinergic synapses of the electric organ of *Torpedo*: a combined biochemical, electrophysiological and morphological study, *J. Neurochem.,* 22 (1974) 435–450.
28 Zimmermann, H. and Whittaker, V.P., Different recovery rates of the electrophysiological, biochemical and morphological parameters in the cholinergic synapses of the *Torpedo* electric organ after stimulation, *J. Neurochem.,* 22 (1974) 1109–1114.
29 Zimmermann, H. and Whittaker, V.P., Morphological and biochemical heterogeneity of cholinergic synaptic vesicles, *Nature,* 267 (1977) 633–635.
30 Zimmermann, H. and Denston, C.R., Recycling of synaptic vesicles in the cholinergic synapses of the *Torpedo* electric organ during induced transmitter release, *Neuroscience,* 2 (1977) 695–714.
31 Zimmermann, H. and Denston, C.R., Separation of synaptic vesicles of different functional states from the cholinergic synapses of the *Torpedo* electric organ, *Neuroscience,* 2 (1977) 715–730.